Polarized Two-photon Absorption Spectra of Naphthalene in Durene Single Crystal with Two Synchronized Tunable Dye Lasers

Naohiko MIKAMI*,† and Hwai-Kwan HONG

Department of Chemistry and Radiation Laboratory, University of Notre Dame, Notre Dame, Indiana 46556, U.S.A.††

(Received February 15, 1979)

Polarized two-photon absorption spectra of naphthalene in a single crystal of durene were observed with one and two beams of tunable dye lasers. Diagonal elements of the two-photon transition tensor were determined by one beam experiments with different incident polarizations on different faces of an oriented single crystal. The off-diagonal elements of the two-photon transition tensor were determined with two synchronized beams of different wavelengths and polarizations on the same sample. It was found that most of the vibronic states have large σ_{LL} consistent with an overall vibronic A_g symmetry and a long axis polarized $^1B_{2u}$ intermediate state. The intermediate states of the two-photon process of the strongest vibronic origin have been discussed on the basis of the observed values of the two-photon transition tensor elements. The band also has a small but non-vanishing off-diagonal tensor element (σ_{LM}). A crystal field perturbation due to reduced site symmetry by a B_{3g} two-photon allowed state is postulated.

Two-photon spectroscopic measurements of polyatomic molecules have become popular for observing new states inaccessible to the usual one-photon spectroscopy. A considerable amount of work has been done on the lowest singlet state of benzene.[1-7] The two-photon excitation spectra of a benzene crystal at very low temperature and of benzene vapor reveal new vibronic structures identified as u-type vibrations in the electronically two-photon forbidden state. In order to determine the symmetry species of these vibrations in the excited state, polarization measurements in the gas phase were performed with high resolution. Unlike one-photon spectroscopy, two-photon spectroscopy has the advantage that the polarization effects can be measured in isotropic media such as gases, since a molecule interacts with two photons simultaneously. Assignments of the vibronic transition in benzene vapor *via* polarization measurements have been carried out by several groups.[4-7]

Similarly, polarization measurements of two-photon spectra in crystals provide us direct and detailed information concerning tensors of two-photon transition amplitudes for crystals or molecules in the crystals. The tensor is composed of nine elements. Each element in the tensor can be determined uniquely by polarization measurements on crystals.[8,9] Studies on the polarized two-photon spectra have been made for crystals of aromatic molecules such as naphthalene,[10] pyrazine[14] and biphenyl.[15] However, the experiments were carried out by using only one exciting beam. Hochstrasser and Sung[12] utilized crystal birefringence to obtain two beams of identical photon energies but different polarizations inside the crystal and were able for the first time to obtain information on both the diagonal and off-diagonal elements of the two-photon transition tensors. If the diagonal elements of the tensor for a particular transition are large as compared with the off-diagonal elements, the two-photon signals are dominated by the absorption of the two photons of the same polarization. The determination of a small off-diagonal contribution due to the absorption of two photons of different polarizations becomes difficult. Thus, a two beam experiment with independent photons in frequencies and polarizations is particularly suitable for the detection of off-diagonal elements of the two-photon transition tensors. The frequencies of the two beams should be so chosen that neither $2\nu_1$ and $2\nu_2$ are in resonance with the transition but $\nu_1+\nu_2$ is. This requires sharp transitions and clear window area. Only mixed crystals at low temperatures such as naphthalene in durene reported here are amenable.

The only experiment using two different light sources on an unisotropic crystal was carried out by Froehlich and Mahr on the single crystal of anthracene.[16] The two beam experiment of the two-photon transition of benzene vapor was carried out by Hampf, Neusser and Schlag.[17]

We have measured polarized two-photon excitation spectra of the lowest singlet excited state of naphthalene in a durene single crystal at very low temperature by using two exciting light beams of different wavelength and polarization. The two-photon spectra of naphthalene in this spectral region has been thoroughly studied in the gas phase[18] and crystalline phase at low temperature.[12,13] The strongest false origin is known to be vibronically induced by a u-type vibration of b_{2u} symmetry in the excited state, all experimental evidence being consistent with this assignment. However, there is some uncertainty as to the mechanism for the appearence of the false origin. Careful polarization measurements of both the single crystals of naphthalene and naphthalene in a durene single crystal by Hochstrasser and Sung[12] shed some light on the nature of intermediate states, crystal field mixing and vibronic coupling in these systems. Our two beam experiment is complimentary to their one beam experiments. The polarization measurements include not only all the possible crystal faces but also new results with two synchronized dye laser beams of different wavelength and polarization. It is thus possible to obtain information on the relative ratio of the individual elements of

† Present address: Department of Chemistry, Faculty of Science, Tohoku University, Sendai 980.

†† The research was supported by the Division of Physical Research of the U. S. Energy Research and Development Administration. This paper is Document No. NDRL-1777 from the Notre Dame Radiation Laboratory.

the two-photon transition tensor. We will discuss the intermediate states of the two-photon process of the strongest vibronic origin and also the crystal field perturbation on two-photon states based on our results for the two-photon transition tensor.

Experimental

Apparatus for the two-photon excitation spectra with two beams of parallel incidence is shown in Fig. 1. Two dye lasers were pumped simultaneously by a nitrogen laser (Molectron UV-1000) with a beam splitter, reflection-transmission ratio being *ca.* 2:3. A home-made dye laser (laser 1) of almost the same design as Molectron DL-200 generated a lasing line with a fixed wavelength. After passing through a 90° prism and an iris, the output beam (beam 1) was polarized horizontally by a Glan-Thompson prism (P_1). A halfwave plate (H) made of thin mica was used in order to change the polarization of beam 1. Suitable selection of the angle between the axis of the plate and the horizontal axis afforded a horizontally or vertically polarized beam without any beam walk-off. A neutral density filter N_1 was used to control the light intensity. Beam 2, frequency of which was tuned continuously and which exits from dye laser 2 (Molectron DL-200), was polarized vertically by another Glan-Thompson prism (P_2). The two beams were adjusted close to each other, the distance between centers being *ca.* 7 mm, and kept parallel to each other by a mirror M_2. Mirrors M_1 and M_2 constitute an optical delay line to synchronize the two light pulses. The two beams were focused onto a sample by a spherical mirror M_3 of 300 mm focal length, spatial matching between the two beams also being accomplished at the same time. As long as the angle between the axis of the incident beam and the normal axis of the mirror is small (<5°), good focusing can be achieved. Polarization of the two beams was carefully checked at the point where the dewar was to be placed. No scrambling of polarization was observed. The sample was held on a rotatable holder and suspended in a sample compartment of a variable temperature cryostat (Cryogenic Associate CT-72) which was cooled by thermal conduction of cool helium gas down to *ca.* 5 K.

The optical arrangement using two beams with 90 degree incidence is shown in Fig. 2. The crystal should be carefully placed at the exact position where the two beams cross each other since only in this small area do we have sufficient intensities in both beams to observe two-photon signals.

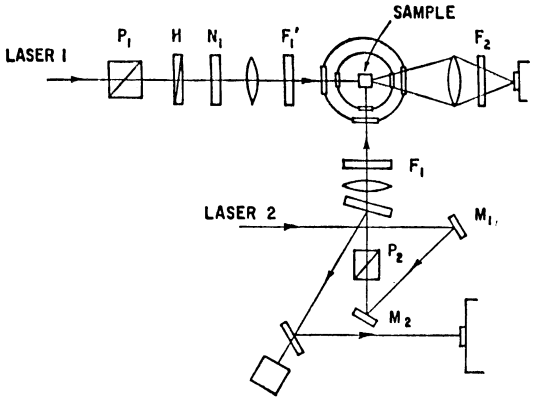

Fig. 2. Optical arrangement for two-photon excitation spectra by two beams with 90 degree incidence.

The fluorescence from the sample was focused onto a small monochromator (Bausch and Lomb) and detected with a photomultiplier (EMI 9635QB) connected to a boxcar integrator (PAR 162). A UV cut-off filter (F_1; Schott GG-22) and a visible cut-off filter (F_2; Corning 7-54) were used to eliminate undesirable photons. The output intensity of beam 2 was monitored by a biplanar photodiode (ITT FW114 with S-20 spectral response). Wavelength of the lasing line was calibrated by a monochromator (Spex 1402).

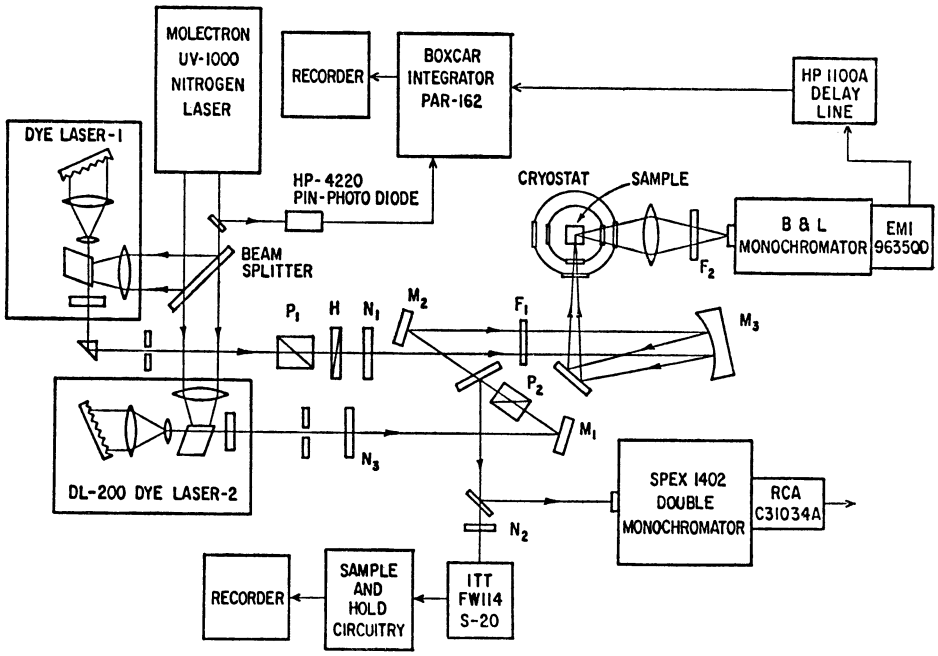

Fig. 1. Experimental set-up for two-photon excitation spectra by two synchronized tunable dye lasers with parallel beam incidence. Notice that the laser beams actually enter the cryostat from the bottom window. The last mirror reflects the beam propagation vector from horizontal to vertical.

Dye solutions were as follows: Cresyl violet perchlorate +Rhodamine-B in EtOH 6600—6200 Å, Rhodamine-B in EtOH 6450—5900 Å, Rhodamine-6G in EtOH 6050—5700 Å. Line width of dye laser 1 in these spectral region was 0.5—0.7 Å, that of laser 2 being less than 0.5 Å.

Naphthalene was purified by fusion with sodium followed by zone refining. Durene (1,2,4,5-tetramethylbenzene) was also purified by the zone melting method. Mixed crystals of durene with *ca.* 1% of naphthalene were grown by the simple Bridgman method. The actual concentration of naphthalene in durene is presumed to be less than 10^{-2} mol/mol. The (ab) crystal plane of durene was cleaved easily. Extinction directions on the (ab) plane were observed under a polarizing microscope. A cube of the crystal with edges parallel to the two extinction axes in the (ab) face (a and b axes) was cut with a razor blade. Examination of the conoscopic pattern of a small flake of the plane showed axis a to differ from axis b. All the directions along the edges of the crystal cube were therefore identified as a, b, and c′ (perpendicular to (ab) face) axes. The X-ray diffraction pattern in precession photographs along each axis confirmed the optical determination of these axes.

One of the principal axes denoted by X is almost parallel to axis a (the angle between it and axis X is known to be −0°54′ in Robertson's axis choice).[19,20] Since axis b coincides with the optical axis Y, all the three crystallographic axes a, b and c′, parallel to the edges of the crystal cube in this work, are parallel to the optical axes X, Y, and Z, respectively. We were able to use the crystallographic axes as reference axes for the polarization experiments.

Results

One Beam Experiment. The two-photon fluorescence excitation spectra of naphthalene in durene crystal with one laser beam was first observed by Hochstrasser, Sung, and Wessel.[10] We have observed almost the same spectra (Figs. 3 and 4). The relative intensities of these absorption peaks are not normalized with respect to the intensity distribution of the dye laser output, since the polarization ratios of the partially polarized laser output varied considerably in the tuning range. The 0-0 transition in this spectral region was

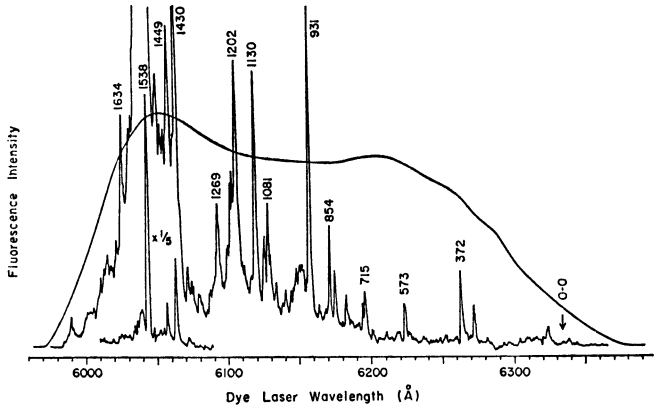

Fig. 3. Unpolarized two-photon excitation spectrum of naphthalene on the (bc′) face of durene crystal at 5 K taken with one laser beam. The smooth curve indicates the intensity distribution of the dye laser (rhodamine-B). The arrow indicates the position of the 0-0 transition.

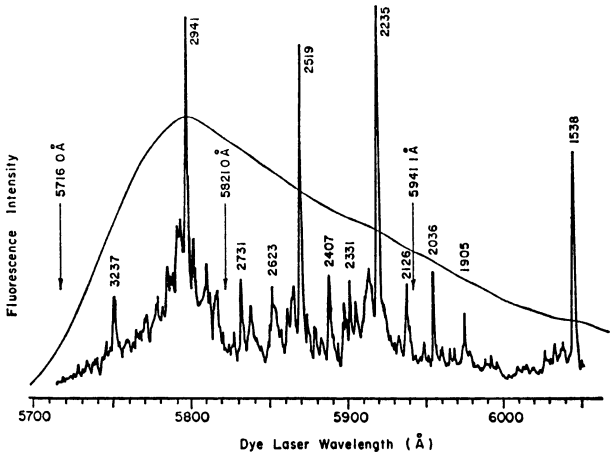

Fig. 4. Unpolarized two-photon excitation spectrum of naphthalene on the (bc′) face of durene crystal at 5 K by using one laser beam. The smooth curve indicates the intensity distribution of the dye laser (rhodamine 6G). The arrows indicate the frequency of the high energy photon in two beam experiments.

measured at 31554 cm^{-1} by McClure.[21] The arrow in Fig. 3 shows the position of the 0-0 transition forbidden in two-photon transition. Energy differences of the main bands from the 0-0 band are summarized in Table 1. Many bands observed in the lower energy side of the strongest false origin at 0+1538 cm^{-1} can be attributed to vibronic bands induced by non-totally symmetric vibrations of u-type. Most bands at the higher energy side of the false origin can be attributed to combinations of u-vibrations and totally symmetric vibrations in the excited state.

The polarized excitation spectra with one beam (Figs. 5—7) are essentially the same as those observed by Hochstrasser and Sung.[12] Due to the wavelength dependence of the polarization of the laser output, the spectra had to be taken in four sections separately for comparison of the two spectra. Usually, one polarized component of the dye laser output is attenuated with respect to the other so that the two polarizations have comparable intensities. The attenuation ratio changes from one spectral section to another, so that one should not compare the intensities of two peaks from different spectral sections. Figure 5 shows a part of the polarized spectra of the strongest vibronic origin at 0+1538 cm^{-1} and a band at 0+1430 cm^{-1} taken on the three principal crystal faces of durene. In the spectra on the (ab) face in which the propagation vector of the incident light is parallel to the c′ axis (k//c′), the peak intensity of the a-polarized spectrum (E//a) of 1538 cm^{-1} is as intense as that of the b-polarized component (E//b). However, in the (ac′) spectra the a-component of the band is more than twice as intense as the c′-component. On the other hand, the 1430 cm^{-1} band is the opposite of that of the 1538 cm^{-1} band in polarization behavior, being predominantly polarized along the c′ axis. Similar characteristics of the polarization spectra in the lower energy regions than the 1430 cm^{-1} band can be seen in Figs. 6 and 7. The polarization ratios are given in Table 2.

Table 1. Observed frequencies of two-photon excitation spectra of naphthalene in durene crystal

λ / Å	$2\tilde{\nu}_{vac}$ / cm^{-1}	$\Delta\tilde{\nu}$[a] / cm^{-1}	Assignment	$\Delta\tilde{\nu}$(obsd)−$\Delta\tilde{\nu}$(calcd)
6232.2	31621	67		
6271.6	31881	327		
6262.7	31926	372	372	
6223.6	32127	573		
6196.2	32269	715	715	
6194.3	32279	725		
6182.9	32338	784		
6173.3	32389	835		
6169.6	32408	854	854	
6155.0	32485	931	931	
6149.7	32513	959	931+28 (lattice mode)	
6139.2	32569	1015		
6132.7	32603	1049		
6126.7	32635	1081	1081	
6124.5	32647	1093		
6117.5	32684	1130	1130	
6104.1	32756	1202	1202	
6091.6	32823	1269	1269	
6079.4	32889	1335		
6074.4	32916	1362		
6071.1	32934	1380		
6061.8	32984	1430	1430	
6058.3	33003	1449		
6049.4	33052	1498		
6042.0	33092	1538	1538	
6037.0	33120	1566	1538+28	
6035.1	33130	1576		
6029.7	33160	1606		
6023.3	33196	1642		
5989.9	33380	1826	1130+697	−1
5975.8	33459	1905	1202+697	+6
5952.5	33590	2036	1538+498	0
5938.3	33670	2116	1130+981	+5
5936.6	33680	2126	1430+697	−1
5917.5	33789	2235	1538+697	0
5912.0	33820	2266	1538+697+28	+3
5903.8	33867	2313		
5900.7	33885	2331	931+1403	−3
5896.9	33907	2353		
5887.4	33961	2407	1430+981	−4
5882.6	33989	2435		
5877.5	34019	2465		
5873.0	34045	2491		
5868.2	34073	2519	1538+981	0
5864.8	34092	2538	1538+981+28	−9
5850.3	34177	2623	1430+498+697	−2
5838.0	34249	2695		
5831.8	34285	2731	1538+498+697	−2
5826.3	34318	2764		
5815.7	34380	2826	1430+2×697	+2
5809.6	34416	2862		
5800.7	34469	2915		
5796.3	34495	2941	1538+1403	0
5792.2	34520	2966	1538+1403+28	−3
5784.0	34569	3015	1538+498+981	−2
5777.0	34610	3056		
5747.0	34791	3237	1538+698+981(?)	+21

a) Frequency difference from the 0-0 transition at 31554 cm^{-1}.[21]

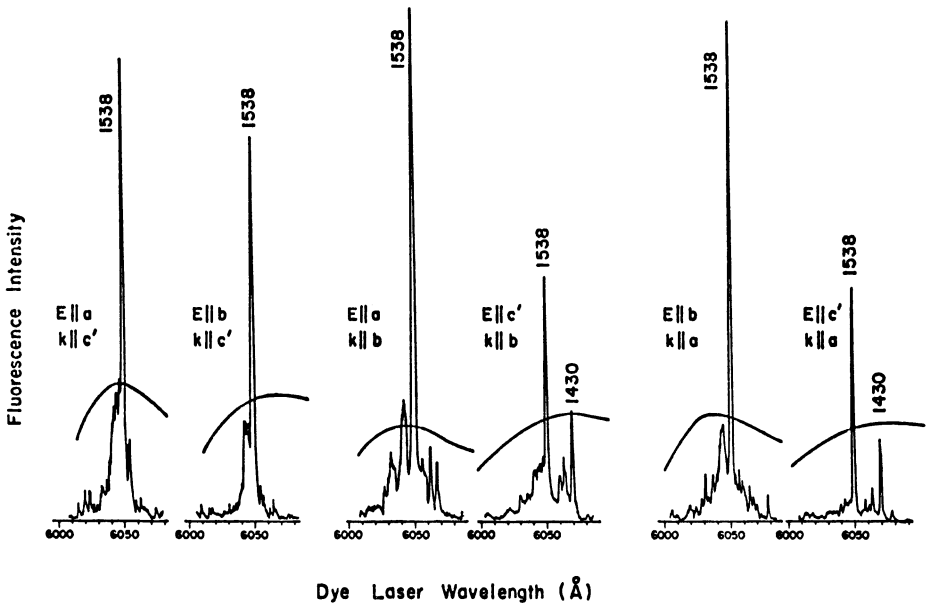

Fig. 5. Polarized two-photon spectra of the strongest vibronic origin in three different crystal faces of durene, with one laser beam. Smooth curves indicate intensity distributions.

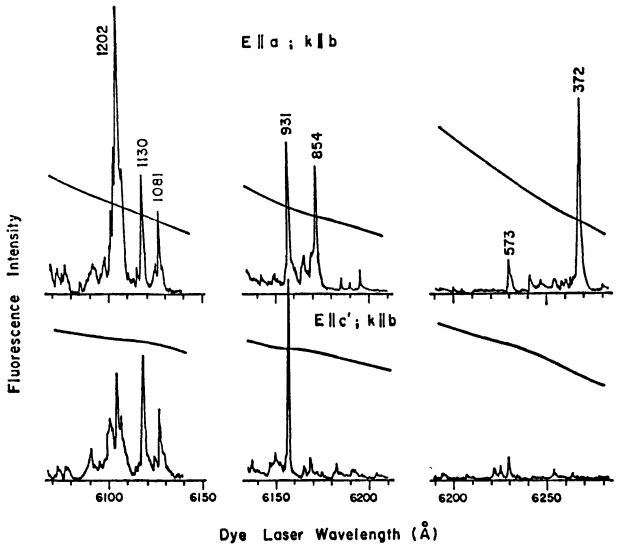

Fig. 6. A part of polarized two-photon excitation spectra in the (ac′) face of durene. Smooth curves indicate dye laser intensity distributions. One cannot compare the relative intensities in different spectral regions.

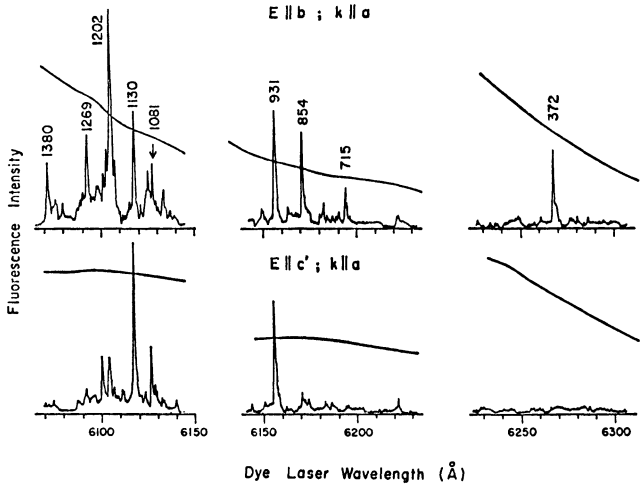

Fig. 7. A part of the polarized two-photon excitation spectra in the (bc′) face of durene. Smooth curves indicate dye laser intensity distributions. One cannot compare the relative intensities in different spectral regions.

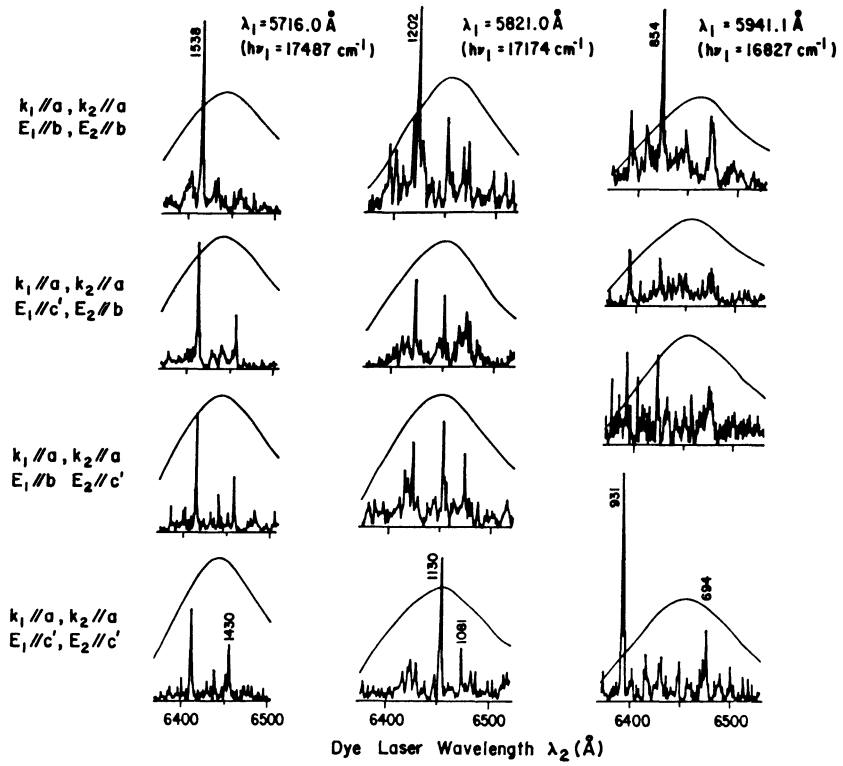

Fig. 8. A part of the polarized two-photon excitation spectra with two dye lasers of different frequencies and different polarizations and parallel beam incidence. The spectra were taken on the (bc′) face of durene at 5 K. k_1, E_1, and λ_1 indicate the k-vector, the polarization and the wavelength of the incident photon with higher energy, respectively. k_2, E_2, λ_2 indicate those of the lower energy photon. One cannot compare the relative intensities in different spectral regions. Smooth curves indicate intensity distributions of dye laser with lower-energy (Cresyl violet+ Rhodamine-B).

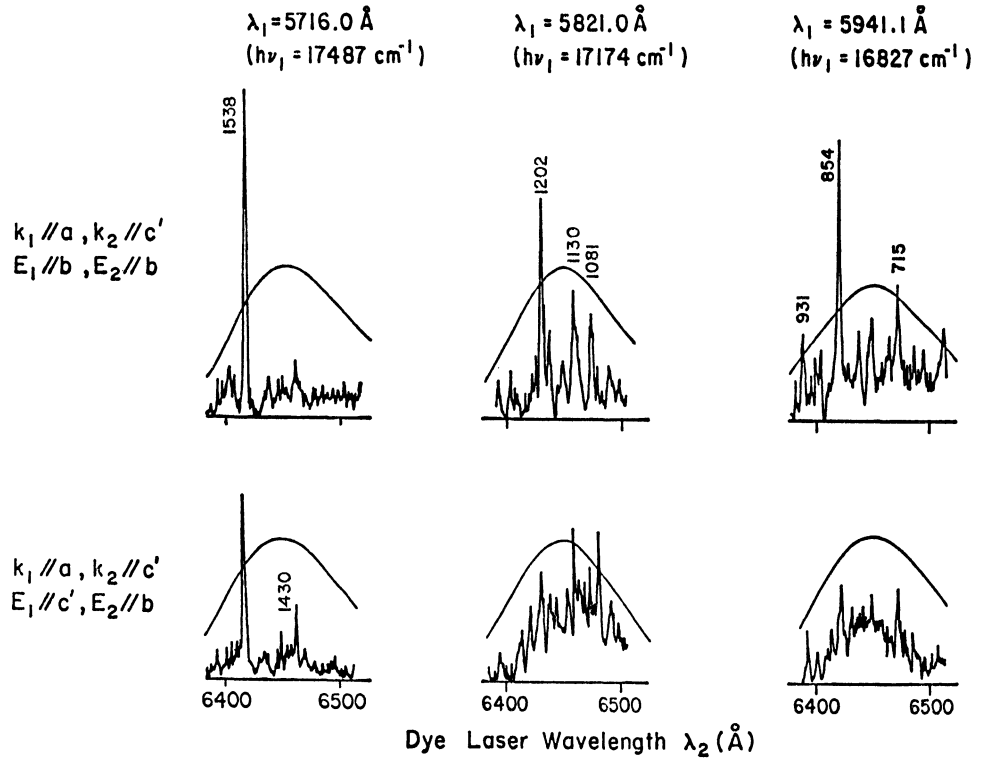

Fig. 9. A part of the polarized two-photon excitation spectra using two beams with 90 degree incidence. k_1, k_2 indicate k-vectors of the high energy photon λ_1 with the polarization E_1 and the lower energy photon λ_2 with the polarization E_2 respectively.

We can distiguish at least three kinds of bands with different polarization behavior (Figs. 5—7). The vibronic bands at 372, 715, 854, 1202, and 1269 cm^{-1} (type I) are polarized predominantly along the a-component on the (ac') spectra and also along the b-component on the (bc') spectra. Another group including 931, 1130, and 1430 cm^{-1} (type III) are apparently polarized along the c'-component in the (ac') or (bc') spectra. The strongest false origin at 1538 cm^{-1} and a band at 1081 cm^{-1} (type II) which are polarized weakly along the a axis in the (ac') plane and also along the b axis in the (bc') plane.

Two Beam Experiment. The excitation spectra taken with two beams of different frequencies and polarizations are shown in Figs. 8 and 9. λ_1 refers to the wavelength of the laser beam with higher energy and λ_2 to that of lower energy photons (Fig. 1). The sum of the frequencies of these two lights should coincide with the excitation energy of the transition. Since the lower frequency photon (λ_2) was tuned in the range where the molecule was not excited by the absorption of the two quanta of λ_2, the two-photon energy of λ_1 should always be higher than the transition energy. Thus, λ_1 beam necessarily induces a constant background on the excitation spectra. However, we were able to find suitable wavelengths of λ_1 to minimize the background (the wavelength λ_1 is indicated by arrow in Fig. 4).

Figure 8 shows the observed spectra using two beams of parallel incidence. The top two spectra in each

Table 2. Observed intensity ratios of the main vibronic bands

$\Delta\tilde{\nu}$ / cm^{-1}	$\left[\frac{I(bb)}{I(c'c')}\right]_1$ a)	$\left[\frac{I(bc')}{I(bb)}\right]_2$ b)	$\left[\frac{I(c'b)}{I(c'c')}\right]_2$ b)	$\left[\frac{I(bb)}{I(c'c')}\right]_2$ b)	$\left[\frac{I(aa)}{I(c'c')}\right]_1$ a)	$\left[\frac{I(ac')}{I(aa)}\right]_2$ b)	$\left[\frac{I(c'a)}{I(c'c')}\right]_2$ b)	$\left[\frac{I(aa)}{I(c'c')}\right]_2$ b)
372	>25	—	—	—	>80	—	—	—
715	7.9	0.48	0.91	1.9	7.7	—	—	—
854	11	0.27	5.0	19	38	—	—	—
931	<1.2	0.82	0.34	0.41	0.31	—	—	—
1081	1.5	0.86	1.27	1.5	3.5	0.68	1.60	2.35
1130	<1.4	0.81	0.62	0.76	2.3	0.88	1.64	1.86
1202	6.7	0.42	1.82	4.5	7.7	1.13	>3.0	>2.65
1269	4.6	0.15	2.78	18	—	—	—	—
1430	0.32	2.69	1.05	0.38	0.84	>1.60	0.67	<0.42
1538	1.8	0.62	1.25	2.0	2.5	0.68	1.57	2.31

a) Value taken from one beam experiment. b) Value taken from two beam experiment.

column were taken by simply changing the polarization of beam 1 without disturbing the optics or changing the sensitivity of the detection system. The lower two spectra were taken after a 90° rotation of the crystal along the axis of incident beams (the incident beams enter the cryostat from the bottom window, see Fig. 1). Thus we can directly measure the ratio for an individual band, $I(\mathrm{bc}')/I(\mathrm{bb})$, by using the normarized peak of the upper two spectra and also $I(\mathrm{c}'\mathrm{b})/I(\mathrm{c}'\mathrm{c}')$ by using the lower two spectra in Fig. 8. We can assume that the middle two spectra, *i.e.* $I(\mathrm{bc}')$ and $I(\mathrm{c}'\mathrm{b})$, are identical when the frequency difference between the photons λ_1 and λ_2 is so small that the asymmetric property of the two-photon transition tensor can be neglected. We can then obtain the polarization ratio $I(\mathrm{bb})/I(\mathrm{c}'\mathrm{c}')$ with two beams on the (bc') plane. Observed polarization ratios in the two beam experiment are summarized in Table 2 together with the ratios in the one beam experiments. The reproduced intensity ratios $I(\mathrm{bb})/I(\mathrm{c}'\mathrm{c}')$ or $I(\mathrm{aa})/I(\mathrm{c}'\mathrm{c}')$ for the two beam experiments are in line with those measured directly from the one beam experiment.

A part of the polarized spectra using two beams with 90 degree incidence is shown in Fig. 9. Each spectrum is similar to its counterpart in Fig. 8. It can be concluded that the polarized spectra do not depend on the direction of propagation of the incident laser beams.

Discussion

Estimation of the Two-photon Transition Tensor. Polarization dependence of two-photon transition can be expressed in terms of a 3×3 tensor. Consider the probability of a two-photon transition i→f. A component of the matrix element of the two-photon transition is expressed as follows:

$$(\sigma^{\mathrm{if}})_{\mathrm{AB}} = \sum_{\mathrm{e}}\left\{\frac{\langle \mathrm{i}|\vec{p}\cdot\hat{e}_{\mathrm{A}}|\mathrm{e}\rangle\langle \mathrm{e}|\vec{p}\cdot\hat{e}_{\mathrm{B}}|\mathrm{f}\rangle}{\Delta E_{\mathrm{ie}}-\hbar\omega_{\mathrm{A}}+i\Gamma_{\mathrm{e}}} + \frac{\langle \mathrm{i}|\vec{p}\cdot\hat{e}_{\mathrm{B}}|\mathrm{e}\rangle\langle \mathrm{e}|\vec{p}\cdot\hat{e}_{\mathrm{A}}|\mathrm{f}\rangle}{\Delta E_{\mathrm{ie}}-\hbar\omega_{\mathrm{B}}+i\Gamma_{\mathrm{e}}}\right\}, \tag{1}$$

where $|\mathrm{e}\rangle$ is an intermediate state for the two-photon process with its excitation energy ΔE_{ie} and a line width Γ_{e}. A and B denote the polarization of the incident photons with energy $\hbar\omega_{\mathrm{A}}$ and $\hbar\omega_{\mathrm{B}}$, respectively. The complete form of the tensor can be expressed by using molecular symmetric axes (L, M, N) as basis axes. We have

$$\sigma^{\mathrm{if}} \equiv \begin{bmatrix} \sigma_{\mathrm{LL}} & \sigma_{\mathrm{LM}} & \sigma_{\mathrm{LN}} \\ \sigma_{\mathrm{ML}} & \sigma_{\mathrm{MM}} & \sigma_{\mathrm{MN}} \\ \sigma_{\mathrm{NL}} & \sigma_{\mathrm{NM}} & \sigma_{\mathrm{NN}} \end{bmatrix}_{\mathrm{if}} \tag{2}$$

Generally, σ^{if} is an asymmetric tensor. It can be split into two parts,[8] symmetric and antisymmetric:

$$\sigma^{\mathrm{if}} = \sigma_{\mathrm{s}}^{\mathrm{if}} + \sigma_{\mathrm{a}}^{\mathrm{if}}$$

$$\sigma_{\mathrm{s}}^{\mathrm{if}} = \begin{bmatrix} \sigma_{\mathrm{LL}} & \frac{(\sigma_{\mathrm{LM}}+\sigma_{\mathrm{ML}})}{2} & \frac{(\sigma_{\mathrm{LN}}+\sigma_{\mathrm{NL}})}{2} \\ \frac{(\sigma_{\mathrm{ML}}+\sigma_{\mathrm{LM}})}{2} & \sigma_{\mathrm{MM}} & \frac{(\sigma_{\mathrm{MN}}+\sigma_{\mathrm{NM}})}{2} \\ \frac{(\sigma_{\mathrm{NL}}+\sigma_{\mathrm{LN}})}{2} & \frac{(\sigma_{\mathrm{NM}}+\sigma_{\mathrm{MN}})}{2} & \sigma_{\mathrm{NN}} \end{bmatrix}_{\mathrm{if}}, \tag{3}$$

$$\sigma_{\mathrm{a}}^{\mathrm{if}} = \begin{bmatrix} 0 & \frac{(\sigma_{\mathrm{LM}}-\sigma_{\mathrm{ML}})}{2} & \frac{(\sigma_{\mathrm{LN}}-\sigma_{\mathrm{NL}})}{2} \\ \frac{(\sigma_{\mathrm{ML}}-\sigma_{\mathrm{LM}})}{2} & 0 & \frac{(\sigma_{\mathrm{MN}}-\sigma_{\mathrm{NM}})}{2} \\ \frac{(\sigma_{\mathrm{NL}}-\sigma_{\mathrm{LN}})}{2} & \frac{(\sigma_{\mathrm{NM}}-\sigma_{\mathrm{MN}})}{2} & 0 \end{bmatrix}_{\mathrm{if}} \tag{4}$$

If the energy separation between the initial state and the intermediate state ΔE_{ie} is large as compared with the incident photon energies, *i.e.* off-resonance condition or energy difference between the two photons $\hbar\omega_{\mathrm{A}}$ and $\hbar\omega_{\mathrm{B}}$ is negligible as compared with the ΔE_{ie}, $\sigma_{\mathrm{a}}^{\mathrm{if}}$ can be neglected. Therefore, σ^{if} will be adequately approximated by the symmetric form $\sigma_{\mathrm{s}}^{\mathrm{if}}$. We assume that the transition tensor is symmetric even in the case of the two beam experiment with different photon energies, because the difference of these photon energies is very small as compared with the ΔE_{ie}.

The electronic state in the crystal can be described in terms of molecular states in the crystal lattice, *i.e.* the oriented gas model. Knowing the direction cosines of the molecular axes in the crystal, we can express the polarization characteristics of the two-photon transition in an oriented crystal in terms of the molecular two-photon transition tensor. The intensity ratio between the two polarized spectra $I(\alpha\beta)$ and $I(\gamma\delta)$ can be written as

$$\frac{I(\alpha\beta)}{I(\gamma\delta)} = \frac{|\sum_{\mathrm{AB}}\sigma_{\mathrm{AB}}\cos\theta_{\alpha}^{\mathrm{A}}\cos\theta_{\beta}^{\mathrm{B}}|^2}{|\sum_{\mathrm{AB}}\sigma_{\mathrm{AB}}\cos\theta_{\gamma}^{\mathrm{A}}\cos\theta_{\delta}^{\mathrm{B}}|^2}, \tag{5}$$

where α, β, or γ, δ denote the crystal axes, and A and B the molecular axes. σ_{AB} denotes the AB elements of molecular tensor of the two-photon transition amplitude in Eq. 2, $\cos\theta_{\alpha}^{\mathrm{A}}$ being the direction cosine between the crystal axis α and molecular axis A. Orientational factor of the two-photon transition of naphthalene in durene crystal can be easily obtained since the guest molecules are known to be embedded substitutionally in the lattice. L and M indicate the molecular long and short axes, respectively, in the molecular plane of naphthalene. a, b, and c' indicate the crystal axes of durene which are very close to the optical axes. Since the projection of axis N, which is perpendicular to the molecular plane, are very similar to those of axis L, we cannot distinguish their contributions. However, the contribution from axis N can be safely neglected since there are no dipole allowed transitions along it for the low-lying electronic states of the molecule. Under these conditions, we can easily find a leading term of the molecular tensor component in the two-photon spectra. As an example,

$$\begin{aligned} I(\mathrm{bb}) &= C\cdot(0.317)\sigma_{\mathrm{LL}}^2 \\ I(\mathrm{c}'\mathrm{c}') &= C\cdot(0.972)\sigma_{\mathrm{MM}}^2 \\ I(\mathrm{c}'\mathrm{b}) &= I(\mathrm{bc}') = C\cdot(0.555)\{\sigma_{\mathrm{LM}}^2+\sigma_{\mathrm{ML}}^2\} \\ I(\mathrm{aa}) &= C\cdot(0.184)\sigma_{\mathrm{LL}}^2 \\ I(\mathrm{ab}) &= I(\mathrm{ba}) = C\cdot(0.241)\sigma_{\mathrm{LL}}^2 \\ I(\mathrm{ac}') &= I(\mathrm{c}'\mathrm{a}) = C\cdot(0.423)\{\sigma_{\mathrm{LM}}^2+\sigma_{\mathrm{ML}}^2\} \end{aligned} \tag{6}$$

where C is a constant.

We can estimate the relative magnitudes of the squared elements of the tensor in the first approxima-

tion. If the relative signs of the elements are known, iterations using Eq. 5 can be employed to obtain more precise values. However, our experimental values are not sufficiently accurate to do so and the signs of the elements are not known. Corrections on the first approximation cannot exceed 10% of the original values and are thus ignored. The relative magnitude of the squared molecular two-photon transition amplitudes are given in Table 3.

Table 3. Relative magnitude of the tensor elements for two-photon transitions

$\frac{\Delta\tilde{\nu}}{\mathrm{cm}^{-1}}$	$\left\|\frac{\sigma_{MM}}{\sigma_{LL}}\right\|^2$	$\left\|\frac{\sigma_{LM}}{\sigma_{LL}}\right\|^2$	Type
715	0.04	0.14	I
854	0.02	0.08	I
931	0.78	0.23	III
1081	0.22	0.25	II
1130	0.42	0.23	III
1202	0.07	0.12	I
1269	0.02	0.04	I
1430	0.86	0.77	III
1538	0.16	0.18	II

We can draw the following conclusions: (1) The gross features of the polarization measurements indicate that σ_{LL} is the predominant tensor element. This might be due to the fact that most intense low-lying transitions of naphthalene are long-axis polarized. Since two-photon transition should gain intensity from one-photon transitions, the behavior is not unexpected. (2) Type I bands can be associated with the smallest σ_{MM}; type II with slightly larger σ_{MM} and type III with even larger σ_{MM}, with respect to σ_{LL}. The naphthalene guest molecules are so oriented that even a small σ_{MM} gives rise to a large $I(c'c')$. (3) The relatively large σ_{LM} is somewhat unexpected. For type I and II bands, all the assignments so far are in line with a b_{2u} vibration in a $^1B_{2u}$ electronic state to yield an overall A_g vibronic state. No σ_{LM} is expected within the oriented gas model. We can either relax the symmetry selection rules by introducing the crystal field perturbations or assume higher order radiation field-molecule coupling schemes. It appears that the former interpretation is more reasonable. (4) Type III bands can be interpreted as either a (LL+MM) mechanism of an A_g vibronic symmetry or LM mechanism of a B_{3g} vibronic symmetry. The crystal field perturbation could be operating here also with the net effect that polarization behavior becomes less distinct.

Assignments for Prominent Lines Based on the Dominant Tensor Elements. Assignments have been made by Hochstrasser and Sung[12] and by Mikami and Ito[13] for the individual vibronic transitions of naphthalene based on polarization experiments on crystals and by Boesel *et al.*[18] for the spectrum in vapor. Let us discuss these assignments (Table 3).

(1) 1538 cm^{-1}: This is the strongest vibronic origin of the spectrum. The dominant tensor element is σ_{LL} of an A_g two-photon tensor, which confirms the results reported by the others 1538 cm^{-1} in this work corresponds to 1540 cm^{-1} in durene crystal and 1542 cm^{-1} in neat crystal given by Hochstrasser and Sung, to 1535 cm^{-1} in pure crystal given by Mikami and Ito, and to 1559 cm^{-1} in vapor spectrum given by Boesel *et al.* The vibrational assignment of this band seems to be well established, *i.e.* 1538 cm^{-1} in the excited state has been assigned to a b_{2u} species which corresponds to 1375 cm^{-1} (ν_{14}) of a b_{2u} type vibration in the ground state. Although this is polarized strongly along the LL-component in the neat crystal, we have observed a non-vanishing amount of MM-component (σ_{MM}) in the durene crystal. In the study by Hochstrasser and Sung the same characteristics have been observed (*cf.* Ref. 12, Table IV) while the ratio of σ_{MM} to σ_{LL} in the neat crystal should be much less than the ratio in durene (*cf.* Ref. 12, Table V). Another remarkable point is existence of the unexpected off-diagonal two-photon tensor element σ_{LM}. This would not be the case on the basis of the assignment described above.

(2) 1430 cm^{-1}: Two-photon tensor shows mixed polarization. Like other type III bands, assignment of this band could not be made unequivocally. This could be attributed to LM-polarization, characteristic of a B_{3g} tensor with a b_{1u} vibration. Hochstrasser and Sung assigned their 1433 cm^{-1} band to a b_{2u} vibration with a dominant MM-component of an A_g tensor. No corresponding band was observed in the gas phase.

(3) 1269 cm^{-1}: This is polarized dominantly in LL-component which means an A_g tensor with a b_{2u} vibration. This agrees with the assignment by Hochstrasser and Sung for their 1276 cm^{-1} band. No corresponding band was observed in vapor.

(4) 1202 cm^{-1}: This polarized in the LL-component of an A_g tensor although an unnegligible amount of LM-component was observed. This corresponds to 1207 cm^{-1} by Hochstrasser and Sung and 1206 cm^{-1} in vapor by Boesel *et al.*, which have also been assigned as an A_g vibronic transition with a b_{2u} vibration.

(5) 1130 cm^{-1}: Mixed components were observed. The polarization characteristics of this band are similar to those of 1430 cm^{-1}. This could be assigned as LM-mechanism of a B_{3g} vibronic state, although an A_g tensor with mixed components (LL+MM) are also possible. Hochstrasser and Sung also observed 1140 cm^{-1} band with a similar polarization behavior to their 1433 cm^{-1}. They pointed out that the appropriate tensor is an A_g type on the basis of polarization in the neat crystal.

(6) 1081 cm^{-1}: The tensor pattern is similar to that of 1538 cm^{-1}. No corresponding band was observed by others.

(7) 931 cm^{-1}: Mixed polarization was observed. The tensor pattern is similar to that of 1430 cm^{-1}. We assigned this to A_g with mixed polarization (LL+MM) confirming the assignment for their 941 cm^{-1} by Hochstrasser and Sung. Boesel *et al.* assigned their 940 cm^{-1} band in vapor spectrum to a B_{3g} vibronic band induced by b_{1u} vibration, and Mikami and Ito also assigned their 901 cm^{-1} band in neat crystal to a B_{3g} state. The discrepancy might be due to the complicated tensor pattern of this band which cannot be clarified by simple one beam experiments.

TABLE 4. ASSIGNMENTS AND MECHANISMS OF TWO-PHOTON TRANSITIONS OF THE MAIN VIBRONIC BANDS (in cm^{-1})

Hochstrasser and Sung[a] (in durene)	Mikami and Ito[b] (in pure crystal)	Boesl, Neusser and Schlag[c] (in gas)	This work (in durene)
390(b_{1u})	365(b_{1u})	355(b_{1u})	372
		592(b_{2u})	573
			715(b_{2u}) LL
863(b_{3u})	847(b_{2u})	865(b_{3u})	854(b_{2u}) LL
941(b_{2u})	901(b_{1u})	940(b_{1u})	931(b_{2u}) LL+MM
	1029(b_{2u})		
1102			1081(b_{2u}) LL
1140(b_{1u})	1107(b_{2u})		1130(b_{2u} or b_{1u}) LL+MM or LM
1194(b_{1u})			
1207(b_{2u})	1203(b_{2u})	1206(b_{2u})	1202(b_{2u}) LL
1276(b_{1u})			1269(b_{2u}) LL
1433(b_{2u})	1397(b_{2u})		1430(b_{1u} or b_{2u}) LM or LL+MM
1506(b_{1u})			
1540(b_{2u})	1535(b_{2u})	1559(b_{2u})	1538(b_{2u}) LL

a) Ref. 12. b) Ref. 13. c) Ref. 18.

(8) 854 cm^{-1}: This band is polarized dominantly along LL-component which corresponds to an A_g tensor, if we assume that the contribution from the N axis of the molecule can be neglected. Hochstrasser and Sung assigned their 863 cm^{-1} in durene to a B_{1g} vibronic band on the basis of the anisotropy of the two-photon signal of the corresponding bands 853 and 857 cm^{-1} in the neat crystal. Boesel *et al.* also assigned their 865 cm^{-1} in vapor spectrum to a B_{1g} state induced by b_{3g} vibration in the excited state. In our analysis we cannot distinguish the difference in polarization characteristics of LL and NN, because of the orientation of the molecule in durene crystal.

(9) 715 cm^{-1}: This is polarized along LL-component. This band might correspond to 727 cm^{-1} in the neat crystal spectra by Hochstrasser and Sung. No corresponding band was observed in vapor.

(10) 372, 573 cm^{-1} and Other Weak Bands: No two beam experiments was carried out on these bands because of weakness of their two-photon signal. The results are summarized in Table 4.

Intermediate States of the Two-photon Processes in the 1538 cm^{-1} Band. The strongest false origin at 1538 cm^{-1} in the spectrum is one of the key bands which characterize the two-photon spectrum in the lowest excited singlet state ($^1B_{2u}$) of naphthalene. The mechanism of the vibronic coupling for this band has been discussed in detail based on the polarization experiment of the neat crystal. It was emphasized that the vibronic coupling between the excited state and the ground state through the b_{2u} vibration of 1538 cm^{-1} is involved.[13] Let us consider the intermediate states for the two-photon transition processes of the band. From Eq. 1 we get the following expressions of the matrix element for the two-photon transition.

$$(\sigma^{gf})_{LL} = \sum_L \left\{ \frac{\vec{\mu}_{gL}^{(1)} \cdot \vec{\mu}_{Lf}^{(2)}}{\Delta E_{gL} - \hbar\omega_1 + i\Gamma_L} + \frac{\vec{\mu}_{gL}^{(2)} \cdot \vec{\mu}_{Lf}^{(1)}}{\Delta E_{gL} - \hbar\omega_2 + i\Gamma_L} \right\}$$
$$(\sigma^{gf})_{MM} = \sum_M \left\{ \frac{\vec{\mu}_{gM}^{(1)} \cdot \vec{\mu}_{Mf}^{(2)}}{\Delta E_{gM} - \hbar\omega_1 + i\Gamma_M} + \frac{\vec{\mu}_{gM}^{(2)} \cdot \vec{\mu}_{Mf}^{(1)}}{\Delta E_{gM} - \hbar\omega_2 + i\Gamma_M} \right\} \quad (7)$$

Where $\vec{\mu}_{gL}^{(1)} \equiv \langle g|\vec{r}\cdot\hat{e}_1|L\rangle$, $\vec{\mu}_{Mf}^{(2)} \equiv \langle M|\vec{r}\cdot\hat{e}_2|f\rangle$ *etc.* L denotes an intermediate state of the two-photon process with B_{2u} symmetry and M a state with B_{1u} symmetry. $\vec{\mu}_{Lf}$, $\vec{\mu}_{Mf}$ denote the transition moment from the intermediate states to the final vibronic level at 1538 cm^{-1} above the origin of the lowest singlet state. We do not known the values of $\vec{\mu}_{Lf}$ or $\vec{\mu}_{Mf}$. However, we adopt the vibronic coupling involving the ground state described above. The transition moment can be estimated from the known values of $\vec{\mu}_{gL}$ or $\vec{\mu}_{gM}$ which are the transition moments from the ground state to the L or M states. The electronic wave function of the vibronic state in the first excited state can be expressed by a linear combination of the zeroth order wave function of the state and that of the ground state with the coupling constant of Herzberg-Teller type along the normal coordinate of the b_{2u} vibration. Transition moment from a higher electronic excited state L or M to the vibronic state expressed by such an approximation can be split into two terms, the transition moment from L or M to the zeroth order first excited state, and that from L or M to the ground state multiplied by a Herzberg-Teller coupling constant. Since the L or M state is an optically allowed state from the ground state and should have an *ungerade* symmetry, the former term in the transition moment would vanish in the framework of approximation. The second term contributes to the transition moment $\vec{\mu}_{Lf}$ or $\vec{\mu}_{Mf}$. We can safely assume that the transition moments from a higher electronic excited state L or M to the vibronic state are proportional to the transition moments from the L or M state to the ground state. Neglecting the difference between $\hbar\omega_1$ and $\hbar\omega_2$ in Eq. 7, we have the following expressions for the two-photon tensor elements:

$$(\sigma^{gf})_{LL} = 2\sum_L \left\{ \left(\frac{H'_{ge}}{\Delta E_{ge}} \right) \cdot \left(\frac{\vec{\mu}_{gL} \cdot \vec{\mu}_{Lg}}{\Delta E_{gL} - \hbar\omega + i\Gamma_L} \right) \right\}$$
$$(\sigma^{gf})_{MM} = 2\sum_M \left\{ \left(\frac{H'_{ge}}{\Delta E_{ge}} \right) \cdot \left(\frac{\vec{\mu}_{gM} \cdot \vec{\mu}_{Mg}}{\Delta E_{gM} - \hbar\omega + i\Gamma_M} \right) \right\} \quad (8)$$

where H'_{ge} denotes the matrix element of the Herzberg-Teller coupling.

By means of the expressions we can estimate $(\sigma_{MM}/\sigma_{LL})^2$ by using the observed values of the oscillator strength f and the excitation energies of the low-lying π-π^* excited states. The values are as follows[22]

$S_1(^1B_{2u}$: L-polarization) $f=0.002$ $\Delta E=32200\ cm^{-1}$
$S_2(^1B_{1u}$: M-polarization) $f=0.18$ $\Delta E=35000$
$S_3(^1B_{2u}$: L-polarization) $f=1.70$ $\Delta E=45300$
$S_4(^1B_{2u}$: L-polarization) $f\approx0.2$ $\Delta E=52500$
$S_5(^1B_{1u}$: M-polarization) $f\approx0.6$ $\Delta E=59800$

Taking 16500 cm^{-1} as the photon energy of the incident photon $\hbar\omega$ and neglecting the line width Γ's, we have 1.7×10^{-8} cm^2 for the $(\sigma)^2_{LL}$ with unit Herzberg-Teller constant. The contribution to the two-photon tensor element arises mainly from S_3 and S_4 with constructive sum. For the MM-component the constructive sum of the contributions from the two M-polarized excited states S_2 and S_5 has also been considered, $(\sigma)^2_{MM}$ being found to be 2.2×10^{-9} cm^2 with the same unit. The calculated ratio $(\sigma_{MM}/\sigma_{LL})^2$ is then 0.13, the value observed being 0.16. In spite of the simple estimation agreement between the estimate and observed values is fairly good. The ratio calculated with a contribution from a single excited state to each component turns out too large or too small as compared with the value obtained. The destructive interference between the contributions in each tensor component from any two excited states can be neglected because neither excited state is below the energy of the incident photon. From the results we conclude that all the low-lying electronic states contribute as the intermediate states for the two-photon transition to the 1538 cm^{-1} vibronic state in the lowest singlet state. This seems to be reasonable since the energies of both incident photons ω_1 and ω_2 in this experiment are far from the excitation energies of the intermediate states, *viz.*, the off-resonance condition in the two-photon absorption processes. In the off-resonance condition all the low-lying electronic states should contribute to the two-photon processes, as in the case of the off-resonance condition in Raman processes.

Crystal Field Effects on the Two-photon Transition. If we assume the oriented gas model for two-photon spectra in the crystal, we should have no off-diagonal matrix element σ_{LM} (and σ_{ML}) of the molecular two-photon tensor of A_g type. However, as shown in Table 3, a considerable amount of off-diagonal component was observed even in A_g vibronic states. For example, the 1538 cm^{-1} band has already been assigned to the A_g vibronic state composed of b_{2u} vibration in the $^1B_{2u}$ electronic state from both crystal and vapor spectra. For the sake of confirmation we have carried out detailed polarization measurement of the band using two beams on the three different crystal faces of durene. The ratios of intensities of different polarizations as compared to the strongest component I(ab) are given in Table 5, together with calculated ratios using the estimated values of the squared ratio of the two-photon tensor elements (Table 3); $\sigma_{LL}=1.00$, $\sigma_{MM}=0.16$, $\sigma_{LM}=0.18$. We see that the estimated values of the squared tensor elements reproduce the polarization ratios for different crystal faces fairly well. The predicted behavior and that of observed polarization of the vibronic states are more or less in agreement.

Table 5. Relative intensities of the strongest false origin at 1538 cm^{-1} in the polarized spectra of different crystal faces

	I(aa)	I(bb)	I(c'c')	I(ab)	I(bc')	I(ac')
Obsd ratio	0.97	0.65	0.38	1.00	0.41	0.68
Calcd ratio	0.38	0.66	0.32	1.00	0.41	0.32

In order to understand the strange polarization effect of the two-photon transition in the crystal, we should take into account the crystal field effect on the molecular states. Group-theoretically the tensor of the molecule embedded in the site of the durene crystal is no longer diagonal since the site symmetry of the crystal is C_i and all the g molecular states fall into A_g symmetry in the C_i site group. In this case three different crystal field mixing processes of the states in the crystal can be considered. (1) Mixing of the normal modes of the molecular vibrations in the crystal due to molecular deformation. For example, the vibrational mode mixing between b_{2u} vibration and b_{1g} vibration causes mixing of the two-photon states of A_g symmetry and of B_{3g} symmetry. In this process, redistribution of the two-photon intensity among all the vibronic states of the same electronic state would take place. This is not very likely since no intense bands with a σ_{LM} component can be identified that can share σ_{LM} with the A_g vibronic state. (2) Mixing among the intermediate states of the two-photon processes is possible. One intermediate state with B_{2u} symmetry (L-polarization), for example, will interact with the other intermediate state with B_{1u} symmetry (M-polarization) in the presence of the crystal field or due to the molecular deformation in the crystal. In this case, the apparent LM-component of the tensor due to the crystal field perturbation V_c can be expressed as

$$(\sigma^{gf})_{LM}=2\sum_L\left\{\frac{\vec{\mu}_{gL}\cdot\sum_M(\lambda_{LM}\cdot\vec{\mu}_{Mf})}{\Delta E_{gL}-\hbar\omega+i\Gamma_L}\right\}+2\sum_M\left\{\frac{\vec{\mu}_{gM}\cdot\sum_L(\lambda_{ML}\cdot\vec{\mu}_{Lf})}{\Delta E_{gM}-\hbar\omega+i\Gamma_M}\right\} \quad (9)$$

where $\lambda_{LM}=\langle L|V_c|M\rangle/\Delta E_{LM}$ stands for the interaction between the intermediate states L and M. Using the same assumption and oscillator strengths for the L or M states employed in the preceding section, we require a very large value of λ_{LM} (more than unity) for any pair of the states L and M to reproduce the observed ratio $(\sigma_{LM}/\sigma_{LL})^2$. Such a large coupling is not likely. (3) The third process is interstate coupling between the vibronic state and other two-photon allowed electronic state with g symmetry. At least two g-electronic states in near UV region have been observed.[11,23] The lower one has been assigned to a B_{3g} electronic state in consideration of theoretical calculations. The other state has been assigned to an A_g electronic state. We can expect the mixing of wave

functions of the vibronic state A_g with that of the electronic B_{3g} and/or of the electronic A_g states. Such a mixing could provide a mechanism for the appearance of σ_{LM} in an A_g vibronic state. The perturbed wave function of the vibronic A_g state in the B_{2u} state (with a reduced symmetry of A) can be found by application of perturbation theory using the crystal flield perturbation V_c and the perturbing electronic state B which has originally a B_{3g} symmetry. Two-photon transition tensor of the true crystalline state of the vibronic A state can be expressed as

$$\begin{bmatrix} \sigma_{LL} & \sigma_{LM} \\ \sigma_{ML} & \sigma_{MM} \end{bmatrix}^{A}_{crystal} = \begin{bmatrix} \sigma_{LL} & 0 \\ 0 & \sigma_{MM} \end{bmatrix}^{A_g}_{mol} + \frac{\langle A|V_c|B\rangle}{\Delta E_{AB}} \begin{bmatrix} 0 & \sigma_{LM} \\ \sigma_{ML} & 0 \end{bmatrix}^{A_{3g}}_{mol} \quad (10)$$

where the perturbation on the ground state is neglected and contributions from axis N are omitted. From Table 3, the ratio of the $|\sigma_{LM}|^2$ to $|\sigma(\text{total})|^2 (=|\sigma_{LL}|^2+2\cdot|\sigma_{LM}|^2+|\sigma_{MM}|^2)$ is found to be 0.12. The strength of the two-photon transition to the B_{3g} electronic state (located at about 44400 cm^{-1}) is about ten times that of the A_g vibronic state.[11] The mixing coefficient, $\langle A|V_c|B\rangle/\Delta E_{AB}$, is therefore estimated to be 0.11 or less. If we take the energy separation between the vibronic state and the B_{3g} state as $\Delta E_{AB}=9300$ cm^{-1}, the interaction energy $\langle A|V_c|B\rangle$ due to the crystal field is estimated to be about 990 cm^{-1}.

In order to ascertain the possibility of the crystal field mixing mechanism (3), there are no other suitable physical quantities in the excited state of the molecule which is directly related to the perturbation. However, if we assume that the stabilization energy of the excited molecular state in the crystal is almost of the same order of magnitude as that of the ground state, we can estimate the order of magnitude of the crystal field effect in the excited state. The total energy of an excited molecule A in a crystal can be written as

$$E_A(\text{crystal}) = E_A(\text{gas}) + \langle A|V_c|A\rangle + \sum_B \frac{|\langle A|V_c|B\rangle|^2}{\Delta E_{AB}}, \quad (11)$$

if we regard the $[E_A(\text{crystal})-E_A(\text{gas})]$ as the heat of sublimation of naphthalene (or durene). We have 6×10^3 cm^{-1}/ molecule for the stabilization energy of a molecule in crystal from the gas phase.[24] Since excited states are generally more polarizable, the value probably represents a lower limit of the stabilization energy of an excited molecule in the crystal. Actually the polarizability of the lowest singlet excited state of naphthalene is slightly larger than that of the ground state.[25,26] Considering only one perturbing state B and taking the value 990 cm^{-1} for $\langle A|V_c|B\rangle$, we have 105 cm^{-1}/ molecule for the second order polarization energy term in Eq. 11, which is one or two orders of magnitude less than the total stabilization energy in the crystal. Although it is not known what percentage of stabilization energy is due to the second order contribution in Eq. 11, the estimated value may not exceed the total second order polarization energy. Our estimate of the strength of crystal field perturbation on the guest molecules appears to be reasonable.

In the absorption study of the first singlet excited state of naphthalene in durene, McClure[27] reported an unexpected polarization behavior of many vibronic bands. Crystal field mixing on the one-photon spectra causes only reduction in the polarization ratios. In order to confirm the effect, very accurate measurements on the relative intensities of the spectra are required. On the other hand, in the two-photon experiments we have more degrees of experimental freedom on the polarization measurements than in the case of one-photon spectra. It is easy to find out the crystal field effects from the unexpected polarization. Two-photon transition tensors depend on more precise electron distributions in the ground and excited states than the one-photon transition dipoles. Crystal perturbation on the molecular wave function will give rise to more effects on the two-photon tensors.

Possibility of Optical Kerr Effect. Another possible cause for the unexpected off-diagonal component of the two-photon transition tensor in the crystal can be attributed to the occurrence of electric field-induced birefringence by optical light beam, *i.e.*, optical Kerr effect.[28] A strong polarized monochromatic laser beam at frequency ν_1 induces birefringence change in a medium so that the other polarized light beam at frequency ν_2 becomes partially depolarized when the two beams pass through the medium simultaneously. Resonance enhancement of the Kerr effect can efficiently depolarize the beam originally polarized. The resonance effect occurs when the photon energy $2\nu_1$, $2\nu_2$, $|\nu_1-\nu_2|$, or $\nu_1+\nu_2$ coincides with the proper molecular transitions. In the case of Raman resonance, *i.e.*, when $|\nu_1-\nu_2|$ corresponds to the molecular vibrational energy of a Raman active mode, this resonance enhancement of the optical Kerr effect has been observed and is known as Raman-induced Kerr effect.[29]. We can expect a similar enhancement effect on the two-photon resonance, when $\nu_1+\nu_2$ matches the energy of a strong two-photon allowed molecular transition. If this is the case, //b-polarization of ν_1 photon produces //b-polarization of ν_2 polarized originally along $\perp$b. As a result, apparent signal I(//b, $\perp$b) is nearly a mixture of I(//b, //b) and I($\perp$b, $\perp$b) factorized by the ratio of the generated light intensity divided by the original intensity. Since the factor is supposed to be very small, the anomalous polarization observed is too large to be explained completely as a result of the effect.

One of the authors (N. M.) wishes to thank Professor M. Ito, Tohoku University, for his encouragement.

References

1) R. M. Hochstrasser, J. E. Wessel, and H. N. Sung, *J. Chem. Phys.*, **60**, 317 (1974).
2) R. M. Hochstrasser, H. N. Sung, and J. E. Wessel, *Chem. Phys. Lett.*, **24**, 7 (1974).
3) L. Wunsch, H. J. Neusser, and E. W. Schlag, *Chem. Phys. Lett.*, **31**, 433 (1975).
4) D. M. Friedrich and W. M. McClain, *Chem. Phys. Lett.*, **32**, 541 (1975).
5) R. G. Bray, R. M. Hochstrasser, and H. N. Sung, *Chem. Phys. Lett.*, **33**, 1 (1975).

6) J. R. Lombardi, R. Wallenstein, T. W. Hänsch, and D. M. Friedrich, *J. Chem. Phys.*, **65**, 2357 (1976).
7) L. Wunsch, F. Metz, H. J. Neusser, and E. W. Schalg, *J. Chem. Phys.*, **66**, 386 (1977).
8) M. Inoue and Y. Toyozawa, *J. Phys. Soc. Jpn.*, **20**, 363 (1965).
9) W. M. McClain, *J. Chem. Phys.*, **55**, 2789 (1971).
10) R. M. Hochstrasser, H. N. Sung, and J. W. Wessel, *Chem. Phys. Lett.*, **24**, 168 (1974).
11) N. Mikami and M. Ito, *Chem. Phys. Lett.*, **31**, 472 (1975).
12) R. M. Hochstrasser and H. N. Sung, *J. Chem. Phys.*, **66**, 3276 (1977).
13) N. Mikami and M. Ito, *Chem. Phys.*, **23**, 141 (1977).
14) P. Esherick, P. Zinsli, and M. A. El-Sayed, *Chem. Phys.*, **10**, 415 (1975).
15) R. M. Hochstrasser and H. N. Sung, *J. Chem. Phys.*, **66**, 3265 (1977).
16) D. Froehlich and H. Mahr, *Phys. Rev. Lett.*, **16**, 895 (1966).
17) W. Hampf, H. J. Neusser, and E. W. Schlag, *Chem. Phys. Lett.*, **46**, 406 (1977).
18) U. Boesl, H. J. Neusser, and E. W. Schlag, *Chem. Phys.* **15**, 167 (1976).
19) M. Robertson, *Proc. R. Soc. London, Ser. A*, **141**, 659 (1933).
20) A. N. Winchell, "The Optical Properties of Organic Compounds," Academic Press, New York (1954), p. 76.
21) D. S. McClure, *J. Chem. Phys.*, **22**, 1668 (1954).
22) J. B. Birks, "Photophysics of Aromatic Molecules," Wiley, (1969), p. 70.
23) A. Bergman and J. Jortner, *Chem. Phys. Lett.*, **26**, 323 (1974).
24) R. S. Bradley and T. G. Cleasby, *J. Chem. Soc.*, **1953**, 1690.
25) T. Mathies and A. C. Albrecht, *J. Chem. Phys.*, **60**, 2500 (1974).
26) H. Meyer, K. W. Schulte, and A. Schweig, *Chem. Phys. Lett.*, **31**, 187 (1975).
27) D. S. McClure, *J. Chem. Phys.*, **24**, 1 (1956).
28) P. D. Maker and R. W. Terhune, *Phys. Rev.*, **137**, A801 (1965).
29) D. Heiman, R. W. Hellwarth, M. D. Levenson, and G. Martin, *Phys. Rev. Lett.*, **36**, 189 (1976).